CORONAVIRUS

Antibody cocktail to SARS-CoV-2 spike protein prevents rapid mutational escape seen with individual antibodies

Alina Baum, Benjamin O. Fulton, Elzbieta Wloga, Richard Copin, Kristen E. Pascal, Vincenzo Russo, Stephanie Giordano, Kathryn Lanza, Nicole Negron, Min Ni, Yi Wei, Gurinder S. Atwal, Andrew J. Murphy, Neil Stahl, George D. Yancopoulos, Christos A. Kyratsous*

Antibodies targeting the spike protein of severe acute respiratory syndrome coronavirus 2 (SARS-CoV-2) present a promising approach to combat the coronavirus disease 2019 (COVID-19) pandemic; however, concerns remain that mutations can yield antibody resistance. We investigated the development of resistance against four antibodies to the spike protein that potently neutralize SARS-CoV-2, individually as well as when combined into cocktails. These antibodies remain effective against spike variants that have arisen in the human population. However, novel spike mutants rapidly appeared after in vitro passaging in the presence of individual antibodies, resulting in loss of neutralization; such escape also occurred with combinations of antibodies binding diverse but overlapping regions of the spike protein. Escape mutants were not generated after treatment with a noncompeting antibody cocktail.

One promising approach to combat the coronavirus disease 2019 (COVID-19) pandemic involves development of antiviral antibodies targeting the spike protein of severe acute respiratory syndrome coronavirus 2 (SARS-CoV-2). The spike protein is a key mediator of viral infectivity required for attachment and entry into target cells, which is achieved by binding the ACE2 receptor (*1*, *2*). A concern for any antiviral therapeutic is the potential for acquiring drug resistance due to the rapid mutation of viral pathogens. Such resistance becomes more obvious when selective pressure is applied in the setting of drug treatment. For example, when HIV drugs were initially used individually, such drug-selected mutations resulted in widespread resistance. The subsequent success of combination therapy for HIV demonstrated that requiring the virus to simultaneously mutate at multiple genetic positions may be the most effective way to avoid drug resistance.

We recently described parallel efforts, using genetically humanized mice and B cells from convalescent humans, to generate a very large collection of highly potent, fully human neutralizing antibodies targeting the receptor-binding domain (RBD) of the spike protein of SARS-CoV-2 (*3*). The prospective goal of generating this very large collection was to select pairs of highly potent individual antibodies that could simultaneously bind the RBD spike, and thus might be ideal partners for a therapeutic antibody cocktail that not only could be an effective treatment, but might also protect against antibody resistance resulting from virus escape mutants that could arise in response to selective pressure from single-antibody treatments.

To assess the efficacy of our recently described antiviral antibodies against the breadth of spike RBD variants represented in publicly available SARS-CoV-2 sequences identified through the end of March 2020 (representing more than 7000 unique genomes), we used the VSV pseudoparticle system expressing the SARS-CoV-2 spike variants. Our top eight neutralizing antibodies maintained their potency against all tested variants (Table 1), demonstrating broad coverage against circulating SARS-CoV-2.

Next, escape mutants were selected under pressure of single antibodies, as well as of antibody combinations, by using a replicating VSV-SARS-CoV-2-S virus (Fig. 1A). We rapidly identified multiple independent escape mutants for each of the four individual antibodies within the first passage (Fig. 1, B and C, and Fig. 2). Some of these mutants became readily fixed in the population by the second passage, representing 100% of sequencing reads, and are resistant to antibody concentrations of up to 50 μg/ml [a factor of ~10,000 to 100,000 greater concentration than half-maximal inhibitory concentration (IC_{50}) against parental virus]. Sequencing of escape mutants (Fig. 2) revealed that single amino acid changes can ablate binding even to antibodies that were selected for breadth against all known RBD variants (Table 1) and that neutralize parental virus at IC_{50} values in the low picomolar range (*3*).

Analysis of 22,872 publicly available unique genome sequences (through the end of May 2020) demonstrated the presence of polymorphisms analogous to two of the escape amino acid residues identified in our study, albeit at an extremely low frequency of one each. Thus, although natural variants resistant to individual antiviral antibodies were not widely observed in nature, these rare escape variants could easily be selected and amplified under the pressure of ongoing antibody treatment. These studies were conducted with a surrogate virus in vitro; one would expect that similar escape mutations may occur with SARS-CoV-2 virus in vivo under the selective pressure of single-antibody treatment. The differential propensity of VSV and SARS-CoV-2 viruses to acquire mutations may affect the speed at which these escape mutants may arise; however, the likelihood of eventual escape remains high.

Next, we evaluated escape after treatment with our previously described antibody cocktail (REGN10987+REGN10933), which was rationally designed to avoid escape through inclusion of two antibodies that bind distinct and non-overlapping regions of the RBD, and thus can simultaneously bind and block RBD function. Attempts to grow VSV-SARS-CoV-2-S virus in the presence of this antibody cocktail did not result in the outgrowth of escape mutants (Table 2, Fig. 1, B and C, and Fig. 2). Thus, this selected cocktail did not rapidly select for mutants, presumably because escape would require the unlikely occurrence of simultaneous viral mutation at two distinct genetic sites, so as to ablate binding and neutralization by both antibodies in the cocktail.

In addition to the above cocktail, we also evaluated escape after treatment with additional combinations (REGN10989+REGN10934 and REGN10989+REGN10987), this time consisting of antibodies that completely or partially compete for binding to the RBD—that is, two antibodies that bind to overlapping regions of the RBD. Under selective pressure of these combination treatments, we observed rapid generation of escape mutants resistant to one combination but not the other (Table 2, Fig. 1, B and C, and Fig. 2). For an antibody cocktail in which the components demonstrate complete competition (REGN10989+REGN10934), a single amino acid substitution was sufficient to ablate neutralization of the cocktail; hence, both of these antibodies require binding to the Glu^{484} residue in order to neutralize SARS-CoV-2. Interestingly, such rapid escape did not occur for a different antibody cocktail in which the components exhibited only partial competition (REGN10989+REGN10987) (*3*); REGN10987 can weakly bind to RBD when REGN10989 is prebound. Thus, even a combination of antibodies that are not selected to simultaneously bind may occasionally resist escape because their epitopes only partially overlap, or because residues that would result in escape are not easily tolerated by the virus and are therefore not readily selected for.

To functionally confirm that the spike protein mutations detected by sequencing are responsible for the loss of SARS-CoV-2 neutralization by the antibodies, we generated

Regeneron Pharmaceuticals Inc., Tarrytown, NY 10591, USA.
*Corresponding author. Email: christos.kyratsous@regeneron.com

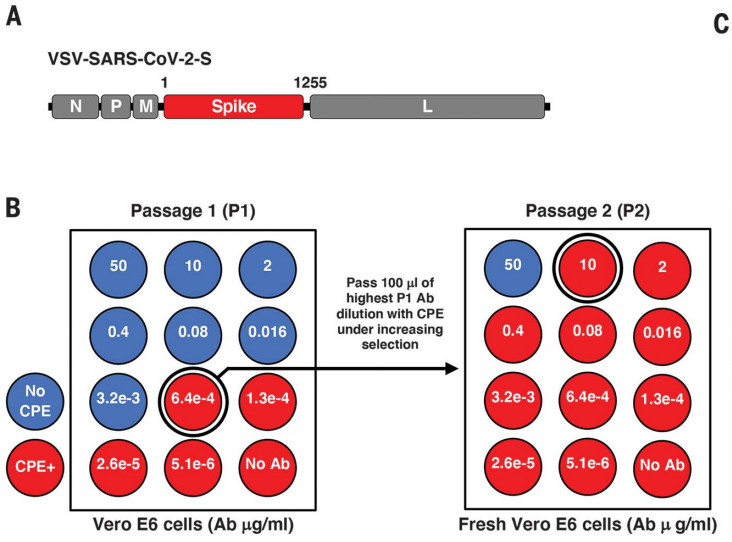

C

Passage	Antibody concentration µg/ml						
P1	50	10	2	0.4	0.08	0.016	No Ab
REGN10989	15%	30%	30%	30%	30%	≥ 90%	≥ 90%
REGN10987	0%	15%	50%	≥ 90%	≥ 90%	≥ 90%	≥ 90%
REGN10933	0%	0%	5%	20%	≥ 90%	≥ 90%	≥ 90%
REGN10934	2-5%	2-5%	30%	50%	≥ 90%	≥ 90%	≥ 90%
REGN10989 + REGN10987	0%	0%	0%	0%	20%	≥ 90%	≥ 90%
REGN10989 + REGN10934	2-5%	2-5%	20%	20%	50%	≥ 90%	≥ 90%
REGN10987 + REGN10933	0%	0%	0%	0%	60%	≥ 90%	≥ 90%
IgG Isotype Control	≥ 90%	≥ 90%	≥ 90%	≥ 90%	≥ 90%	≥ 90%	≥ 90%
P2	50	10	2	0.4	0.08	0.016	No Ab
REGN10989	≥ 90%	≥ 90%	≥ 90%	≥ 90%	≥ 90%	≥ 90%	≥ 90%
REGN10987	5%	40%	≥ 90%	≥ 90%	≥ 90%	≥ 90%	≥ 90%
REGN10933	70%	80%	≥ 90%	≥ 90%	≥ 90%	≥ 90%	≥ 90%
REGN10934	80%	≥ 90%	≥ 90%	≥ 90%	≥ 90%	≥ 90%	≥ 90%
REGN10989 + REGN10987	0%	0%	0%	0%	0%	0%	50%
REGN10989 + REGN10934	≥ 90%	≥ 90%	≥ 90%	≥ 90%	≥ 90%	≥ 90%	≥ 90%
REGN10987 + REGN10933	0%	0%	0%	0%	0%	60%	≥ 90%
IgG Isotype Control	≥ 90%	≥ 90%	≥ 90%	≥ 90%	≥ 90%	≥ 90%	≥ 90%

Fig. 1. Escape mutant screening protocol. (**A**) Schematic of the VSV-SARS-CoV-2-S virus genome encoding residues 1 to 1255 of the spike protein in place of the VSV glycoprotein. N, nucleoprotein; P, phosphoprotein; M, matrix; L, large polymerase. (**B**) A total of 1.5×10^6 plaque-forming units (pfu) of the parental VSV-SARS-CoV-2-S virus was passed in the presence of antibody dilutions for 4 days on Vero E6 cells. Cells were screened for virus replication by monitoring for virally induced cytopathic effect (CPE). Supernatants and cellular RNAs were collected from wells under the greatest antibody selection with detectable viral replication (circled wells; ≥20% CPE). For a second round of selection, 100 µl of the P1 supernatant was expanded for 4 days under increasing antibody selection in fresh Vero E6 cells. RNA was collected from the well with the highest antibody concentration with detectable viral replication. The RNA was deep-sequenced from both passages to determine the selection of mutations resulting in antibody escape. (**C**) The passaging results of the escape study are shown with the qualitative percentage of CPE observed in each dilution (red, ≥20% CPE; blue, <20% CPE). Black-bordered boxes indicate dilutions that were passaged and sequenced in P1 or sequenced in P2. A no-antibody control was sequenced from each passage to monitor for tissue culture adaptations.

Table 1. Anti-SARS-CoV2 spike mAbs demonstrate broad neutralization across SARS-CoV-2 spike RBD variants. Eight anti-spike antibodies were tested against 16 SARS-CoV-2 spike protein RBD variants identified from viral sequences circulating through the end of March 2020. The listed variants were encoded into pVSV-SARS-CoV-2-S (mNeon) pseudoparticles, and neutralization assays were performed in Vero cells. IC_{50}(M) values are shown for each variant. For all variants, no neutralization was observed with hIgG1 isotype control. Amino acid abbreviations: A, Ala; D, Asp; E, Glu; F, Phe; G, Gly; H, His; I, Ile; K, Lys; L, Leu; N, Asn; P, Pro; Q, Gln; R, Arg; S, Ser; T, Thr; V, Val; Y, Tyr.

	Anti-SARS-CoV-2 spike monoclonal antibodies							
Variants	**REGN10989**	**REGN10987**	**REGN10933**	**REGN10934**	**REGN10964**	**REGN10954**	**REGN10984**	**REGN10986**
Wild-type	7.23×10^{-12}	4.06×10^{-11}	4.28×10^{-11}	5.44×10^{-11}	5.70×10^{-11}	9.22×10^{-11}	9.73×10^{-11}	9.91×10^{-11}
Q321L	1.46×10^{-11}	5.02×10^{-11}	6.85×10^{-11}	6.84×10^{-11}	5.65×10^{-11}	2.32×10^{-10}	2.75×10^{-10}	2.06×10^{-10}
V341I	1.61×10^{-11}	3.38×10^{-11}	3.37×10^{-11}	7.42×10^{-11}	1.13×10^{-10}	2.52×10^{-10}	2.49×10^{-10}	1.92×10^{-10}
A348T	7.33×10^{-12}	2.98×10^{-11}	4.13×10^{-11}	1.42×10^{-10}	3.52×10^{-11}	1.84×10^{-10}	2.01×10^{-10}	1.03×10^{-10}
N354D	1.14×10^{-11}	2.68×10^{-11}	5.89×10^{-11}	9.76×10^{-11}	1.93×10^{-10}	2.84×10^{-10}	2.64×10^{-10}	2.49×10^{-10}
S359N	4.30×10^{-12}	2.41×10^{-11}	2.12×10^{-11}	3.04×10^{-11}	6.83×10^{-11}	1.09×10^{-10}	1.23×10^{-10}	8.91×10^{-11}
V367F	1.33×10^{-11}	1.78×10^{-11}	2.40×10^{-11}	3.20×10^{-11}	8.92×10^{-11}	1.29×10^{-10}	1.53×10^{-10}	1.49×10^{-10}
K378R	1.21×10^{-11}	2.40×10^{-11}	3.52×10^{-11}	4.65×10^{-11}	6.19×10^{-11}	1.65×10^{-10}	1.88×10^{-10}	1.54×10^{-10}
R408I	1.09×10^{-11}	1.71×10^{-11}	1.98×10^{-11}	2.75×10^{-11}	4.96×10^{-11}	9.88×10^{-11}	1.35×10^{-10}	6.14×10^{-11}
Q409E	2.12×10^{-11}	4.06×10^{-11}	5.65×10^{-11}	5.94×10^{-11}	6.61×10^{-11}	2.64×10^{-10}	1.52×10^{-10}	1.95×10^{-10}
A435S	1.10×10^{-11}	3.88×10^{-11}	4.71×10^{-11}	8.07×10^{-11}	7.90×10^{-11}	2.11×10^{-10}	2.18×10^{-10}	1.51×10^{-10}
K458R	7.51×10^{-12}	1.68×10^{-11}	3.43×10^{-11}	3.46×10^{-11}	5.46×10^{-11}	1.45×10^{-10}	1.59×10^{-10}	1.00×10^{-10}
I472V	2.27×10^{-11}	4.18×10^{-11}	9.17×10^{-11}	9.40×10^{-11}	1.01×10^{-10}	3.44×10^{-10}	2.61×10^{-10}	2.24×10^{-10}
G476S	6.80×10^{-12}	1.86×10^{-11}	1.41×10^{-10}	3.51×10^{-11}	3.42×10^{-11}	1.83×10^{-10}	2.10×10^{-10}	1.13×10^{-10}
V483A	8.78×10^{-12}	2.60×10^{-11}	1.54×10^{-11}	4.43×10^{-11}	4.50×10^{-11}	1.12×10^{-10}	1.71×10^{-10}	9.70×10^{-11}
Y508H	1.71×10^{-11}	2.75×10^{-11}	4.77×10^{-11}	6.73×10^{-11}	1.02×10^{-10}	2.05×10^{-10}	2.83×10^{-10}	2.01×10^{-10}
H519P	4.51×10^{-12}	2.20×10^{-11}	3.03×10^{-11}	3.56×10^{-11}	4.45×10^{-11}	1.40×10^{-10}	1.08×10^{-10}	6.14×10^{-11}

	Position in genome	3299	3312	3853	4326	4407	4411	4425	4435	4442	4527	4531	4533	4545	4546	4554	5040	5122	5130	5137	5383	5412	6460
	Position in spike gene	222	235	776	1249	1330	1334	1348	1358	1365	1450	1454	1456	1468	1469	1477	1963	2045	2053	2060	2306	2335	3383
	Reference nucleotide	T	T	C	A	A	T	A	A	G	G	G	T	T	T	C	C	G	C	T	G	C	T
	Variant nucleotide	A	A	A	G	C	C	G	T	T	A	A	G	C	C	A	T	A	A	G	A	A	C
	Position in protein	**74**	**79**	**259**	**417**	**444**	**445**	**450**	**453**	**455**	**484**	**485**	**486**	**490**	**490**	**493**	**655**	**682**	**685**	**687**	**769**	**779**	**1128**
	Ref Residue	**N**	**F**	**T**	**K**	**K**	**V**	**N**	**Y**	**L**	**E**	**G**	**F**	**F**	**F**	**Q**	**H**	**R**	**R**	**V**	**G**	**Q**	**V**
	Variant Residue	**K**	**I**	**K**	**E**	**Q**	**A**	**D**	**F**	**F**	**K**	**D**	**V**	**L**	**S**	**K**	**Y**	**Q**	**S**	**G**	**E**	**K**	**A**
	Inoculum	0%	0%	0%	0%	0%	0%	0%	0%	0%	0%	0%	0%	0%	0%	0%	37%	16%	0%	1%	0%	0%	0%
PASSAGE 1	**10933 0.4ug/ml**	0%	0%	0%	12%	0%	0%	0%	29%	16%	0%	0%	11%	0%	0%	3%	51%	18%	0%	31%	11%	0%	0%
PASSAGE 1	**10934 2ug/ml**	0%	0%	0%	0%	3%	0%	34%	0%	0%	14%	0%	0%	0%	43%	0%	63%	43%	3%	0%	0%	0%	0%
PASSAGE 1	**10987 2ug/ml**	0%	0%	0%	0%	30%	36%	0%	0%	0%	0%	0%	0%	0%	0%	0%	54%	22%	29%	1%	0%	0%	0%
PASSAGE 1	**10989 10ug/ml**	0%	0%	0%	0%	0%	0%	0%	0%	0%	99%	0%	0%	0%	0%	0%	99%	2%	0%	0%	0%	15%	0%
PASSAGE 1	**10989 0.08ug/ml**	0%	0%	0%	0%	0%	0%	0%	0%	0%	25%	8%	0%	19%	14%	11%	67%	28%	0%	9%	0%	0%	0%
PASSAGE 1	**10987/33 0.08ug/ml**	0%	0%	0%	0%	0%	0%	0%	0%	0%	0%	0%	0%	0%	0%	0%	49%	26%	1%	3%	1%	0%	0%
PASSAGE 1	**10989/34 0.08ug/ml**	0%	0%	0%	0%	0%	0%	0%	0%	0%	51%	0%	0%	0%	22%	0%	76%	23%	0%	2%	0%	0%	0%
PASSAGE 1	**10989/87 0.08ug/ml**	0%	0%	0%	0%	0%	0%	0%	0%	0%	2%	0%	0%	0%	0%	0%	32%	27%	1%	3%	1%	0%	0%
PASSAGE 1	**Isotype Control 50ug/ml**	0%	0%	0%	0%	0%	0%	0%	0%	0%	0%	0%	0%	0%	0%	0%	61%	28%	0%	4%	0%	0%	0%
PASSAGE 1	**Virus Only**	0%	0%	0%	0%	0%	0%	0%	0%	0%	0%	0%	0%	0%	0%	0%	64%	27%	0%	4%	0%	0%	0%
PASSAGE 2	**10933 50ug/ml**	0%	0%	0%	0%	0%	0%	0%	10%	0%	0%	0%	88%	0%	0%	0%	1%	90%	0%	15%	87%	0%	0%
PASSAGE 2	**10934 50ug/ml**	0%	0%	0%	0%	0%	0%	95%	0%	0%	6%	0%	0%	0%	1%	0%	10%	93%	0%	0%	0%	0%	0%
PASSAGE 2	**10987 10ug/ml**	0%	0%	0%	0%	45%	41%	0%	0%	0%	0%	0%	0%	0%	0%	0%	50%	6%	47%	0%	0%	0%	0%
PASSAGE 2	**10989 50ug/ml**	0%	0%	0%	0%	0%	0%	0%	0%	0%	100%	0%	0%	0%	0%	0%	100%	0%	0%	0%	0%	20%	0%
PASSAGE 2	**10987/33 10ug/ml**	ND	ND	ND	ND	ND	ND	ND	ND	ND	ND	ND	ND	ND	ND	ND	ND	ND	ND	ND	ND	ND	ND
PASSAGE 2	**10989/34 50ug/ml**	0%	0%	0%	0%	0%	0%	0%	0%	0%	100%	0%	0%	0%	0%	0%	93%	11%	0%	0%	0%	0%	0%
PASSAGE 2	**10989/87 10ug/ml**	ND	ND	ND	ND	ND	ND	ND	ND	ND	ND	ND	ND	ND	ND	ND	ND	ND	ND	ND	ND	ND	ND
PASSAGE 2	**Isotype control 50ug/ml**	16%	13%	10%	0%	0%	0%	0%	0%	0%	0%	0%	0%	0%	0%	0%	54%	50%	0%	8%	0%	0%	4%
PASSAGE 2	**Virus Only**	8%	8%	22%	0%	0%	0%	0%	0%	0%	0%	0%	0%	0%	0%	0%	28%	83%	0%	7%	0%	0%	8%

Frequency < 10% | Frequency 10% < x< 50% | Frequency > 50%

Fig. 2. Deep sequencing of passaged virus identifies escape mutations. VSV-SARS-CoV-2-S virus was mixed with anti-spike monoclonal antibodies (mAb), individually or in combination. Viral RNA from wells with the highest mAb concentration and detectable CPE on passage 1 or passage 2 (collected 4 days after infection) was isolated and RNA-seq analysis was performed to identify changes in spike protein sequence relative to input virus. For passage 2, viral RNA was isolated and sequenced from wells with high mAb concentrations (>10 μg/ml) with subsequently validated escape; if no validated escape was seen at these high mAb concentrations and no virus was grown, ND indicates that no virus RNA was isolated. All mutated amino acid residues within the spike protein are shown. The specific condition (concentration in μg/ml) of the well that was selected for sequencing is shown in the left column (see Fig. 1 for outline of the experiment). Red boxes highlight residues that were mutated relative to input virus under each condition specified in the left column. Percentages of sequencing reads that contained the respective mutant sequence are identified. Residues mapping to the RBD are highlighted in blue.

VSV-SARS-CoV-2 spike pseudoparticles expressing the individual identified spike mutations. These pseudoparticles were used in neutralization assays with single- and multiple-antibody treatments, and IC_{50} values were calculated (Table 2 and fig. S1). As expected, pseudoparticles with amino acid mutations that were selected by passaging the virus in the presence of the four single antibodies, as well as of the REGN10989 +REGN10934 competing antibody cocktail, were sufficient to completely eliminate or greatly decrease the ability of these treatments to neutralize in these assays. Single escape mutants that were detected at low frequency in early passages in virus populations generated by two antibodies [e.g., Lys^{444} → Gln (K444Q) by both REGN10934 and REGN10987] but were fixed in the later passage by only one of these antibodies (REGN10987) were able to ablate neutralization by both treatments. This suggests that antibodies can drive virus evolution and escape in different directions. However, if two antibodies have partially overlapping binding epitopes, then escape mutants fixed in the virus population by one can result in the loss of activity of the other; this highlights the risks of widespread use of single-antibody treatments. Notably, the REN10987 +REGN10933 antibody cocktail—which consists of two antibodies that can simultaneously bind to two independent epitopes on the RBD—retained its ability to neutralize all identified mutants, even those that were selected for by single treatment with one of its components.

In our sequencing of passaged virus pools, we also identified multiple mutations outside of the RBD, most of which were present at various abundances within control samples, including the original inoculum and virus-only passages (Fig. 2). The most abundant of these mutations [His^{655} → Tyr (H655Y) and Arg^{682} → Gln (R682Q)] are near the S1′/S2′ cleavage site within the spike protein and contain residues within the multibasic furin-like cleavage site. Mutations and deletions in this region have been identified with tissue culture–passaged VSV-SARS-CoV-2-S as well as SARS-CoV-2 viruses and likely represent tissue culture adaptations (*4*, *5*).

Because RNA viruses are well known to accumulate mutations over time, a concern for any antiviral therapeutic is the potential for selection of treatment-induced escape mutants. A common strategy to safeguard against escape to antibody therapeutics involves selection of antibodies binding to conserved epitopes;

Table 2. Neutralization potency of individual anti-spike antibodies and antibody combinations against pseudoparticles encoding individual escape mutants: IC_{50} summary. Escape mutations identified by RNA-seq analysis within the RDB domain were cloned and expressed on pseudoparticles to assess their impact on mAb neutralization potency. Boxes in boldface highlight conditions that resulted in a decrease in IC_{50} of at least 1.5 log units relative to wild-type pseudoparticles or loss of neutralization. NC indicates that IC_{50} could not be calculated because of poor neutralization ability. Reduction in IC_{50} of less than 1 log unit can be seen in mAb combination conditions where one of the mAbs has no potency (e.g., K444Q and REGN10933/10987). See fig. S1 for full neutralization curves.

	Anti-SARS-CoV-2 spike monoclonal antibodies						
Escape mutants	**REGN10989**	**REGN10987**	**REGN10933**	**REGN10934**	**REGN10933/10987**	**REGN10989/10934**	**REGN10989/10987**
Wild-type	7.27×10^{-12}	3.65×10^{-11}	5.57×10^{-11}	5.99×10^{-11}	3.28×10^{-11}	8.27×10^{-12}	1.22×10^{-11}
K417E	2.49×10^{-11}	3.10×10^{-11}	**8.33×10^{-9}**	2.70×10^{-11}	4.15×10^{-11}	2.64×10^{-11}	2.72×10^{-11}
K444Q	2.47×10^{-11}	**NC**	7.81×10^{-11}	**5.38×10^{-9}**	1.23×10^{-10}	4.19×10^{-11}	4.82×10^{-11}
V445A	2.65×10^{-11}	**NC**	8.82×10^{-11}	1.42×10^{-10}	1.54×10^{-10}	4.08×10^{-11}	5.74×10^{-11}
N450D	4.10×10^{-11}	**1.20×10^{-9}**	7.60×10^{-11}	**NC**	1.88×10^{-10}	6.04×10^{-11}	5.37×10^{-11}
Y453F	2.77×10^{-11}	1.04×10^{-10}	**NC**	2.17×10^{-10}	1.15×10^{-10}	3.52×10^{-11}	2.41×10^{-11}
L455F	1.77×10^{-11}	3.87×10^{-11}	**NC**	4.34×10^{-11}	5.87×10^{-11}	1.96×10^{-11}	1.70×10^{-11}
E484K	**NC**	6.25×10^{-11}	**1.13×10^{-9}**	**NC**	6.19×10^{-11}	**NC**	1.88×10^{-10}
G485D	**NC**	2.34×10^{-11}	2.05×10^{-10}	4.47×10^{-11}	4.71×10^{-11}	1.19×10^{-10}	4.58×10^{-11}
F486V	**NC**	3.16×10^{-11}	**NC**	3.50×10^{-11}	8.8×10^{-11}	1.29×10^{-10}	6.96×10^{-11}
F490L	**3.10×10^{-9}**	3.56×10^{-11}	4.53×10^{-11}	**1.94×10^{-9}**	3.64×10^{-11}	**2.50×10^{-9}**	8.37×10^{-11}
F490S	**2.23×10^{-10}**	4.42×10^{-11}	6.63×10^{-11}	**8.91×10^{-9}**	3.4×10^{-11}	**4.2×10^{-10}**	6.58×10^{-11}
Q493K	**NC**	4.19×10^{-11}	**NC**	3.45×10^{-10}	3.24×10^{-11}	**4.55×10^{-10}**	5.94×10^{-11}

however, this strategy may not suffice. Although some informed analysis can be made regarding epitope conservation based on sequence and structural analysis (*6*), the possibility of escape still exists under strong selection pressure. Indeed, escape studies performed with anti-influenza hemagglutinin stem binding antibodies have shown that escape mutants can arise despite high conservation of the stem epitope between diverse influenza subtypes, with some escape mutations arising outside of the antibody epitope region (*7*, *8*). Antibodies that demonstrate broad neutralization across multiple species of coronaviruses, and thus may be targeting more conserved residues, have not been shown to be immune to escape upon selective pressure. In addition, their neutralization potency is orders of magnitude lower than that of the most potent neutralizing antibodies specific for SARS-CoV-2 (*6*, *9*–*11*). Neutralization is thought to be the key mechanism of action of anti-coronavirus spike antibodies and has previously been shown to correlate with efficacy in animal models (*12*), and may therefore prove to be the most important driver of initial clinical efficacy. However, as demonstrated with our single-antibody escape studies, even highly potent neutralization does not protect against the rapid generation of viral escape mutants, and escape remains a major concern with individual antibody approaches.

Our data strongly support the notion that cocktail therapy may provide a powerful way to minimize mutational escape by SARS-CoV-2; in particular, our studies point to the potential value of antibody cocktails in which two antibodies were chosen so as to bind to distinct and non-overlapping regions of the viral target (in this case, the RBD of the spike protein), and thus require the unlikely occurrence of simultaneous mutations at two distinct genetic sites for viral escape. A clinical candidate selection criterion for broad potency that includes functional assessment against naturally circulating sequence variants, as well as inclusion of multiple antibodies with non-overlapping epitopes, may provide enhanced protection against loss of efficacy. Future in vivo animal and human clinical studies will need to pay close attention to the possible emergence of escape mutants and potential subsequent loss of drug efficacy.

REFERENCES AND NOTES

1. R. Yan *et al*., *Science* **367**, 1444–1448 (2020).
2. Q. Wang *et al*., *Cell* **181**, 894–904.e9 (2020).
3. J. Hansen *et al*., Studies in humanized mice and convalescent humans yield a SARS-CoV-2 antibody cocktail. *Science* 10.1126/science.abd0827 (2020).
4. S.-Y. Lau *et al*., *Emerg. Microbes Infect.* **9**, 837–842 (2020).
5. M. E. Dieterle *et al*., A replication-competent vesicular stomatitis virus for studies of SARS-CoV-2 spike-mediated cell entry and its inhibition2020).
6. D. Pinto *et al*., *Nature* 10.1038/s41586-020-2349-y (2020).
7. K. Tharakaraman, V. Subramanian, D. Cain, V. Sasisekharan, R. Sasisekharan, *Cell Host Microbe* **15**, 644–651 (2014).
8. K. L. Prachanronarong *et al*., *J. Virol.* **93**, e01639-18 (2019).
9. S. J. Zost *et al*., Potently neutralizing human antibodies that block SARS-CoV-2 receptor binding and protect animals2020).
10. D. F. Robbiani *et al*., Convergent Antibody Responses to SARS-CoV-2 Infection in Convalescent Individuals2020).
11. Y. Cao *et al*., *Cell* 10.1016/j.cell.2020.05.025 (2020).
12. K. E. Pascal *et al*., *Proc. Natl. Acad. Sci. U.S.A.* **112**, 8738–8743 (2015).

ACKNOWLEDGMENTS

We thank K. Tramaglini for program management, J. Hansen for help with manuscript preparation, and E. Scolnick for useful discussions. **Funding:** A portion of this project has been funded in whole or in part with federal funds from the Department of Health and Human Services, Office of the Assistant Secretary for Preparedness and Response, Biomedical Advanced Research and Development Authority, under OT number HHS0100201700020C. **Author contributions:** A.B., B.O.F., E.W., and C.A.K. conceptualized and designed experiments; B.O.F., E.W., K.E.P., V.R., and S.G. performed research; A.B., B.O.F., E.W., K.E.P., V.R., S.G., G.S.A., A.J.M., N.S., G.D.Y., and C.A.K. analyzed data; R.C., K.L., N.N., M.N., and Y.W. prepared sequencing libraries and performed bioinformatics analysis; A.B., G.D.Y., and C.A.K. wrote the paper; and C.A.K. acquired funding. **Competing interests:** Regeneron authors own options and/or stock of the company. This work has been described in one or more pending provisional patent applications. A.J.M., N.S., G.D.Y., and C.A.K. are officers of Regeneron. **Data and materials availability:** Antibody sequences have been deposited to GenBank and are available in (*3*). Regeneron materials described in this manuscript may be made available to qualified, academic, noncommercial researchers through a material transfer agreement upon request at https://regeneron.envisionpharma.com/vt_regeneron/. For questions about how Regeneron shares materials, use the following email address: preclinical.collaborations@ regeneron.com. This work is licensed under a Creative Commons Attribution 4.0 International (CC BY 4.0) license, which permits unrestricted use, distribution, and reproduction in any medium, provided the original work is properly cited. To view a copy of this license, visit https://creativecommons.org/licenses/by/4.0/. This license does not apply to figures/photos/artwork or other content included in the article that is credited to a third party; obtain authorization from the rights holder before using such material.

SUPPLEMENTARY MATERIALS

science.sciencemag.org/content/369/6506/1014/suppl/DC1
Materials and Methods
Fig. S1
References (*13*–*19*)

30 May 2020; accepted 11 June 2020
Published online 15 June 2020
10.1126/science.abd0831

Science

Antibody cocktail to SARS-CoV-2 spike protein prevents rapid mutational escape seen with individual antibodies

Alina Baum, Benjamin O. Fulton, Elzbieta Wloga, Richard Copin, Kristen E. Pascal, Vincenzo Russo, Stephanie Giordano, Kathryn Lanza, Nicole Negron, Min Ni, Yi Wei, Gurinder S. Atwal, Andrew J. Murphy, Neil Stahl, George D. Yancopoulos and Christos A. Kyratsous

Science **369** (6506), 1014-1018.
DOI: 10.1126/science.abd0831originally published online June 15, 2020

An antibody cocktail against SARS-CoV-2

There is an urgent focus on antibodies that target the severe acute respiratory syndrome coronavirus 2 (SARS-CoV-2) viral spike and prevent the virus from entering host cells. Hansen *et al.* generated a large panel of antibodies against the spike protein from humanized mice and recovered patients. From this panel, they identified several neutralizing antibodies, including pairs that do not compete for binding to the receptor binding domain. Baum *et al.* focused in on four of these antibodies. All four are effective against known spike variants. However, by growing a pseudovirus that expresses the spike in the presence of individual antibodies, the authors were able to select for spike mutants resistant to that antibody. In contrast, escape mutants are not selected when pseudovirus is grown in the presence of pairs of antibodies that either do not compete or only partially compete for binding to the RBD. Such a pair might be used in a therapeutic antibody cocktail.

Science, this issue p. 1010, p. 1014